Drought explains variation in the radial growth of white spruce in western Canada

Lei Chen[1,2], Jian-Guo Huang[1,*], Kenneth J. Stadt[3], Philip G. Comeau[4], Lihong Zhai[1], Andria Dawson [5], Syed Ashraful Alam[1, 6]

[1] Key Laboratory of Vegetation Restoration and Management of Degraded Ecosystems, Provincial Key Laboratory of Applied Botany, South China Botanical Garden, Chinese Academy of Sciences, Guangzhou 510650, China

[2] Graduate School of Environmental Science, Hokkaido University, N19W8, Sapporo 060-0819, Japan

[3] Forest Management Branch, Sustainable Resource Development, Edmonton, Alberta, Canada

[4] Department of Renewable Resources, University of Alberta, Edmonton, Alberta, Canada

[5] Department of Geosciences, University of Arizona, Tucson, Arizona, 85721, USA

[6] Department of Physics, P.O. Box 48, FI-00014, University of Helsinki, Finland

*Corresponding author: Jian-Guo Huang

Tel: +86 20 37264225; Fax: +86 20 37264153; E-mail: huangjg@scbg.ac.cn

Abstract

Many studies have already addressed the existence of unstable and nonlinear relationships between radial growth of white spruce (*Picea glauca*) and climate variables in boreal forests along the high latitudes (> 60° N). However, along the mid-latitudes, the climate-growth relationship is still poorly understood. In this study, we used a network of ring-width chronologies from 40 white spruce sites along a wide latitudinal gradients from 52° N to 58° N in Alberta, Canada and attempted to understand the complicated response of tree growth to climatic variables and to identify the main limiting factor for the radial growth of white spruce. We combined the empirical linear statistics with the process-based Vaganov-Shashkin Lite (VS-Lite) model requiring only latitude, month mean temperature, and monthly total precipitation information together to better clarify growth-climate relationship. The linear statistical methods indicated that the previous summer temperature imposed a strong negative impact on the radial growth of white spruce while the precipitation and climate moisture index in prior and current summer both had significant positive effects on the radial growth. Similarly, the VS-Lite model showed that the radial growth of white spruce was limited by soil moisture, and temperature-induced drought is the main limiting factor for the radial growth of white spruce. Furthermore, climate-growth relationship varied along different elevations, latitudes, and growing degree days (GDD > 5℃). The radial growth of white spruce in northern stands is often more strongly limited by temperature-induced drought due to the higher temperature and lower precipitation. As the global climate change is in progress, we suggest that more large-scale and

continuous investigations are needed to address the spatial variation in growth-climate relationship due to the temperature-induced drought.

Keywords: Boreal forest, drought, radial growth, spatial variation, western Canada, white spruce

1. Introduction

The global surface temperature increased approximately 0.85 °C from 1880 to 2012, and the period from 1983 to 2012 is thought to be the warmest 30-year period of the last 14 centuries in the Northern Hemisphere (IPCC, 2014). It is not well understood how these dramatic changes in climate will affect terrestrial biomes (Ma et al., 2012). The largest of these terrestrial biomes is the boreal forest, which is predominantly distributed across northern Eurasia and North America , and covers 11% of the earth's land surfaces (Dixon et al., 1994; Lindahl et al., 2007). Climate warming will not only influence the function and structure of these boreal forests but also may affect the frequency and severity of abiotic and biotic feedbacks of boreal forests, including outbreaks of forest insects, droughts and wild fires (Stocks et al., 1998; Volney and Fleming, 2000; Kasischke and Stocks, 2012; Price et al., 2013). Therefore, it is critical to understand the response of boreal tree species to climate warming for better predicting potential changes and monitoring in boreal forest ecosystems.

Tree rings provide a high-resolution proxy of climate, and have been successfully used by many studies to reconstruct past climatic change (Mann et al., 2002; Esper et al., 2002; Cook et al., 2004; D'Arrigo et al., 2006; D'Arrigo et al., 2008), and to better understand the relationship between tree growth and climate (Hughes et al., 2010; Speer, 2010; Fritts, 2001). Traditional statistical calibration methods assume a linear relationship between tree growth and climatic factors that is constant through time (Jones et al., 2009; Tolwinski-Ward et al., 2011). As a result of climate warming over the last few decades, various studies (D'Arrigo et al., 2008; Esper and Frank, 2009; Zhang and Wilmking, 2010; Visser et al., 2010) have considered the existence of unstable and nonlinear relationships between tree growth and climate. In particular, it has been shown that white spruce (*Picea glauca* (Moench) Voss) has a complex nonlinear response to climate, at least in parts of Alaska and Yukon, Canada (Wilmking et al., 2004; D'Arrigo et al., 2004; Lloyd et al., 2013). For example, many studies have demonstrated a reduction in the sensitivity of the growth of white spruce to temperature in high altitude boreal forests, especially in Alaska and northern Canada (Jacoby and D'Arrigo, 1995; Lloyd and Fastie, 2002; Wilmking et al., 2004; Andreu-Hayles et al., 2011; Porter and Pisaric, 2011; Chavardès et al., 2013; Lloyd et al., 2013), which is referred to as the divergence problem (D'Arrigo et al., 2008). Except for the temporal change in the climate-growth relationship, the response of radial growth to climate variables also varied along latitudinal gradients in boreal forests (Mäkinen et al., 2002; Huang et al., 2010; Lloyd et al., 2011). Therefore, large spatial scale tree-ring study is needed to clearly address how radial growth responds to climatic factors.

The process-based Vaganov–Shashkin (VS) model that estimates tree-ring growth from environmental inputs has the ability to resolve the non-stationary and nonlinear feature of the climate-growth relationship (Vaganov et al., 2006; Vaganov et al., 2011; Zhang et al., 2011; Touchan et al., 2012). However, the application of the VS model is limited due to its complex structure and required parameter inputs. Tolwinski-Ward et al. (2011) proposed a simplified version of the VS model (VS-Lite), which only requires latitude, monthly temperature and precipitation as inputs. Recent studies have shown that the nonlinear VS-Lite model can capture the growth trajectories of tree-ring series for a variety of environmental conditions and species (Tolwinski-Ward et al., 2011; Breitenmoser et al., 2014). Although the nonlinear response of white spruce growth to climate has been investigated in several high-latitude boreal forests, the climate-growth relationship of white spruce in mid-latitude forests is still poorly understood.

In this study, we used a network of ring-width chronologies from 40 white spruce sites in the boreal forest along mid-latitudinal gradient from 52° N to 58° N in Alberta, Canada. The objectives of this study were to: (1) clarify the response of the radial growth of white spruce to climate variables by comparing the results of traditional empirical linear function analysis and growth estimates from the VS-Lite model, (2) investigate the potential spatial variability in the radial growth of white spruce along the latitudinal gradient. As the western Canadian boreal forest is sensitive to climate change (Peng et al., 2011), in which elevations, latitudes and site effects could lead to spatial variability in climate change (Gewehr et al., 2014), we hypothesized that impacts of drought on the radial growth of white spruce could also vary along latitudinal gradients.

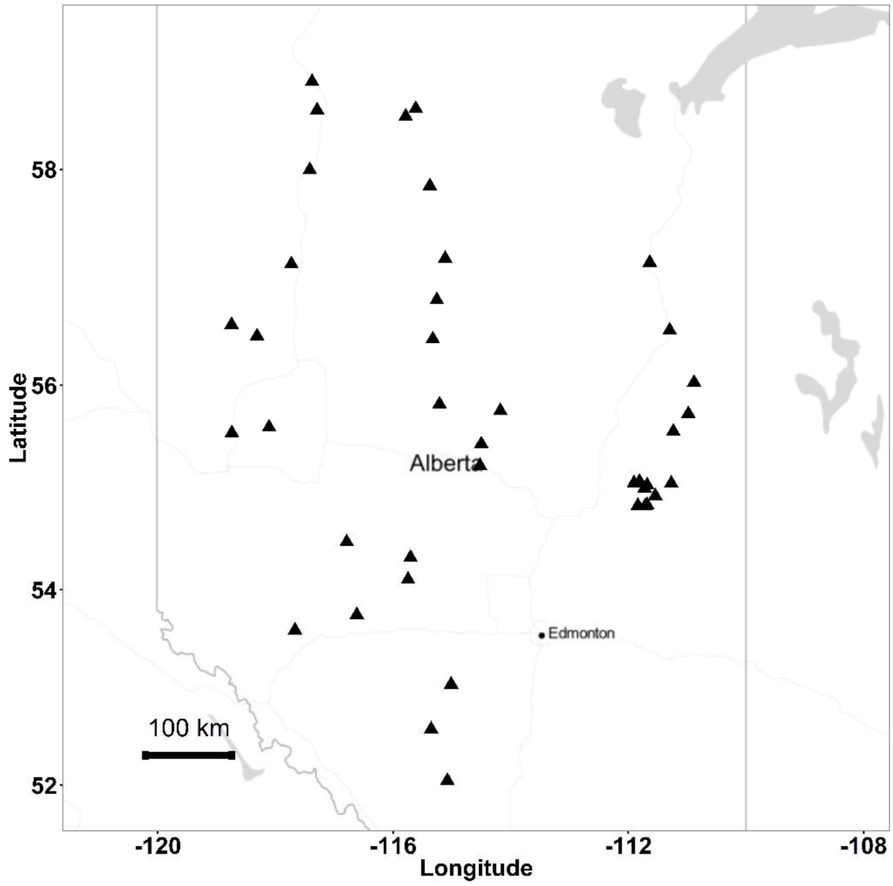

Fig. 1 Locations of the study sites (40 white spruce stands).

2. Materials and methods

2.1 Study area

The study area is located within the mixedwood forests in Alberta, Canada, which covers 75% of the forested area in the province. The dominant species in these forests are white spruce, trembling aspen (*Populus tremuloides* Michx.), balsam poplar

(*Populus balsamifera* L.), paper birch (*Betula papyrifera* Marshall), and balsam fir [*Abies balsamea* (L.) Mill.] (Cumming et al., 2000; Stadt et al., 2007). In addition, Lodgepole pine (*Pinus contorta* Douglas ex Loudon) exists within these mixed forests. Forty sample sites were distributed throughout these regions (Fig. 1), which are under typically dry continental climate conditions. The monthly mean temperature and precipitation from 1930 to 2010 were around 1 °C and 460 mm, respectively (Appendix S1). The main soil types were brunisols and orthic gray luvisols (Beckingham et al., 1996).

2.2 Climate data

The interpolated climate data during the period of 1930-2010 for all the 40 sites were generated using ANUSPLIN (version 4.3) incorporated thin plate-smoothing splines to develop continuous climate surfaces across space based on the limited observed data (Hutchinson, 2004). In this study, the climate variables used include monthly mean temperature (*T*), monthly total precipitation, and growing degree days (GDD > 5°C). The climate moisture index (CMI) (Hogg, 1994; Hogg, 1997) has been successfully applied to predict impacts of drought on aspen forests in western Canada (Hogg et al., 2005; Hogg et al., 2008; Michaelian et al., 2011; Hogg et al., 2013). Therefore, the CMI was also calculated to explore the potential effect of drought on the radial growth of white spruce.

2.3 Tree-ring data

We randomly sampled accessible white spruce dominated mixedwood stands where over 2/3 trees were white spruce, the stand age ranged from 25 to 100 years according to the Phase 3 inventory database (AESRD, 2012). An average of 10 trees were sampled from each site. Trees for tree-ring analyses were either cored or felled. A disk of each sampled tree was collected from stump height (0.3 m). In addition, two 5.1 mm increment cores were collected at 1.3 m height from each sampled tree.

In the laboratory, all tree-ring increment cores were dried and polished with successively finer grits of sandpaper. All tree ring samples were visually crossdated, then measured using a Velmex measuring system with 0.001 mm resolution. Visual cross-dating was verified using COFECHA (Holmes, 1983). Age- and size-related growth trends were removed by detrending raw tree-ring series using a spline with a 50% frequency response (Cook and Kairiukstis, 1990). Standardized tree-ring series often contain low-frequency variation, such as biological persistence. An autoregressive (AR) model was used to remove the low-frequency persistence and enhance the residual common signal. Residual chronologies were developed using a biweight robust mean to reduce the effect of outliers. The chronology was constructed using the dplR package (Bunn, 2008) of R (R Core Team, 2015). In total, 40 white spruce residual ring-width chronologies were constructed.

2.4. Climate-growth analysis

2.4.1 Traditional statistical analysis

The climate-growth relationship was assessed by comparing climate data to the residual chronologies both in a correlation analysis and with a linear mixed model. Temperature and precipitation from previous May to August of the current growing season were tested. In the correlation analysis, climate variables were correlated with residual chronologies. Bootstrapping was used to test the significance of Pearson's correlation values and increase the reliability. Then the linear regression was used to explore the variation in the correlation coefficients along different elevations, latitudes, and growing degree days (GDD > 5℃).

Linear mixed model was used to analyze the effects of climate variables on white spruce growth. The linear mixed model is written as

$$W_{ij} = b_0 + b_1 x_{ij} + m_{i1} + m_{i2} x_{ij} + e_{ij},$$

where W_{ij} and x_{ij} represent the ring width of residual chronologies and the climate variables for site *i* and year *j*; b_0 and b_1 are the fixed effects; m_{i1} and u_{i2} are the random intercept and random slope; $e_{ij} \sim N(0, s^2)$ are the errors in the within-site measurement, m_{i1}, m_{i2} and e_{ij} are assumed to be independent. Precipitation and temperature were entered into the models as fixed effects, while differences of precipitation and temperature within each site were used as the random slopes. Linear mixed model parameters were estimated using the lme4 package (Bates et al., 2014) of R (R Core Team, 2015).

2.4.2 The VS-Lite model

Table 1. Parameters of the VS-Lite model

Temperature response parameters		Value
Threshold temp. for $g_T > 0$	T_1	[1 °C, 9 °C]
Threshold temp. for $g_T = 1$	T_2	[10 °C, 24 °C]
Moisture response parameters		
Threshold soil moist. for $g_M > 0$	M_1	[0.01, 0.035]
Threshold soil moist. for $g_M = 1$	M_2	[0.1, 0.7]
Soil moisture parameters		
Runoff parameter 1	a	0.093 month^{-1}
Runoff parameter 2	m	5.8
Runoff parameter 3	m	4.886
Max moisture held by soil	$W_{\max}$	0.8 v/v
Min moisture held by soil	$W_{\min}$	0.01 v/v
Root (bucket) depth	d_r	1000 mm
Integration window parameters		
Integration start month	I_0	-4
Integration start month	I_f	12

A complete description of the VS-Lite model can be found in the (Tolwinski-Ward et al., 2011). The total radial growth for month i is determined by insolation-related growth g_E, temperature-related growth g_T and soil moisture-related growth g_M, where

$$G(i) = g_E(i)^* \min\{g_T(i), g_M(i)\} \quad (1)$$

Annual growth is calculated by the integrating monthly growth for a calendar year. The parameter $g_E(i)$ is the ratio of the mean monthly day length to that in the summer solstice month, for a given month *i*, and $g_T(i)$ and $g_M(i)$ are calculated according to the following formulas:

$$g_T(i) = \begin{cases} 0 & \text{if} \quad T_i \le T_1 \\ \frac{T_i - T_1}{T_2 - T_1} & \text{if} \quad T_1 < T_i \le T_2 \\ 1 & \text{if} \quad T_i > T_2 \end{cases} \qquad (2),$$

$$g_M(i) = \begin{cases} 0 & \text{if} \quad M_i \le M_1 \\ \frac{M_i - M_1}{M_2 - M_1} & \text{if} \quad M_1 < M_i \le M_2 \\ 1 & \text{if} \quad M_i > M_2 \end{cases} \qquad (3).$$

where T_i and M_i are the temperature and soil moisture values for month *i*, and T_1, T_2, M_1 and M_2 are user-specified the thresholds of temperatures and soil moistures. The VS-Lite model requires latitude, monthly mean temperature and total precipitation as inputs to simulate the growth of tree-ring width in response to soil moisture and temperature. The fitted results of the VS-Lite model are only sensitive to the four parameters: T_1, T_2, M_1 and M_2, which determine the nonlinear tree-ring growth responds to temperature and moisture. The parameters used here, as listed in Table 1, are the same as those published previously (Tolwinski-Ward et al., 2011; Breitenmoser et al., 2014). A Bayesian estimation method was used for the estimation of parameters of the model (Tolwinski-Ward et al., 2013), The Bayesian estimation method assumes the priors of the parameters (T_1, T_2, M_1 and M_2) are uniform distributions and the medians of the posterior distributions are used as the estimated values.

3. Results

3.1 Statistical parameters of the chronologies

Chronology lengths ranged from 28 to 81 years (Appendix S2). The mean ± SD tree-ring width of the chronologies was 1.18 ± 0.76 mm for all the 40 sites. In addition, both positive and negative values of the skew and the first order autocorrelation existed among the chronologies (Appendix S2).

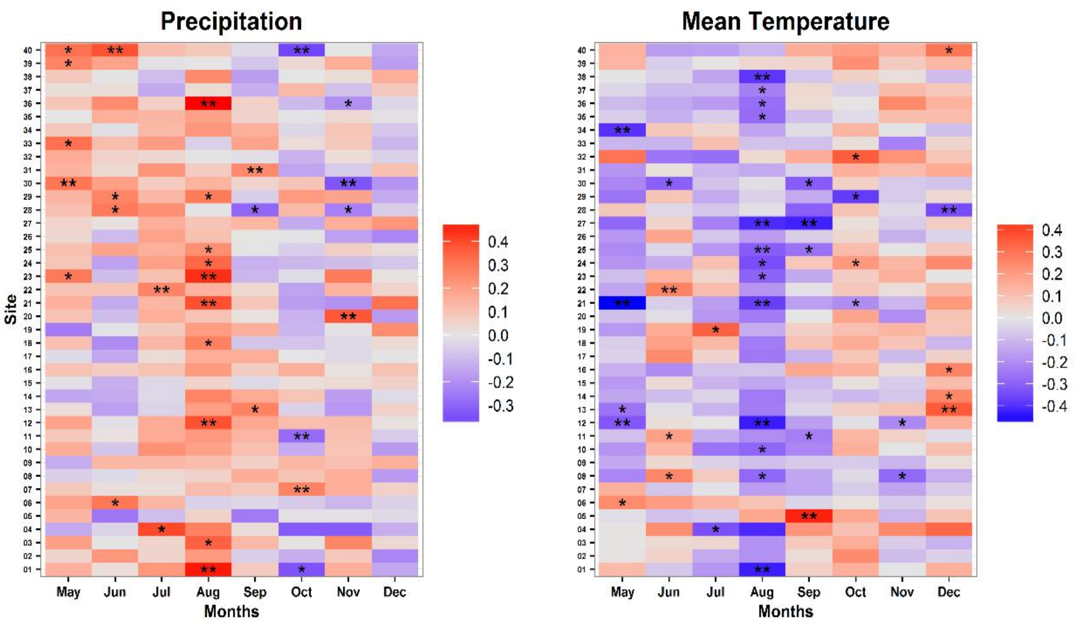

Fig. 2 Bootstrapped correlation coefficients of radial growth and the climate variables of the previous year. One asterisk and two asterisks represent $p<0.05$, $p<0.01$, respectively.

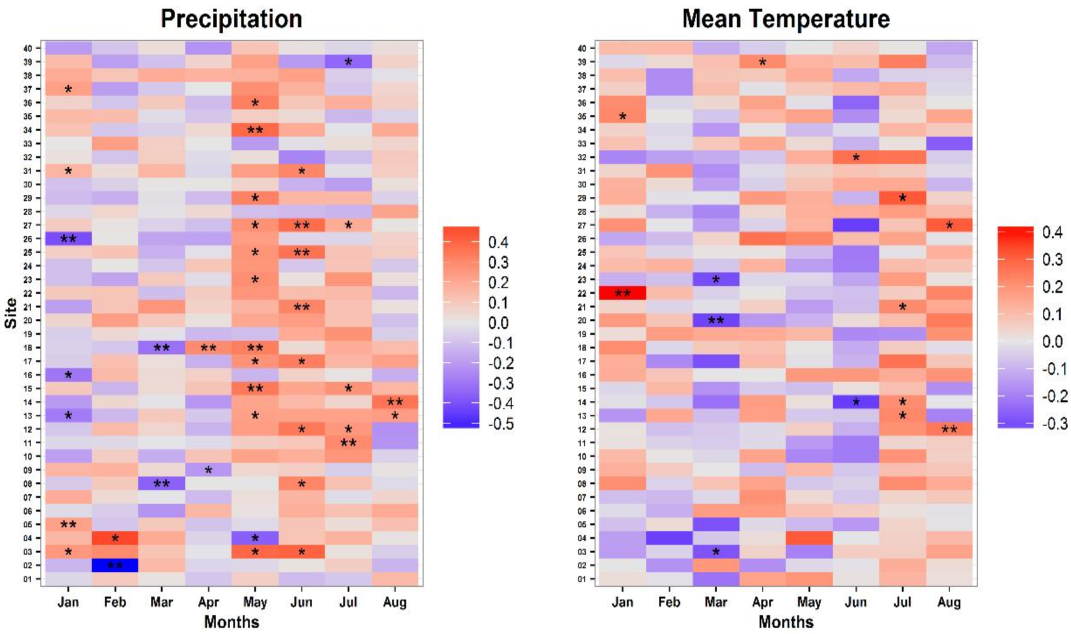

Fig. 3 Bootstrapped correlation coefficients of radial growth and the climate variables of the current year. One asterisk and two asterisks represent *p*<0.05, *p*<0.01, respectively.

3.2 Response of tree-ring growth to climate variables

3.2.1 Correlation analysis

In general, radial growth of white spruce was negatively correlated with summer temperatures of the previous year (Fig. 2). Results indicated that the radial growth in four sites showed significant negative response to the temperature of previous May and the radial growth in 13 sites was significantly negatively correlated with the temperature of previous August (Fig. 2). In contrast, radial growth often positively correlated with the temperature during the period between October and January although only a few significant responses were found (Figs. 2 and 3). In current growing season, radial growth often negatively correlated with the mean temperature in July with four significant cases (Fig. 3).

The radial growth of white spruce in 10 sites was significantly positively correlated with previous August precipitation (Fig. 2). Then the strong positive response to precipitation gradually declined and even became negative (Fig. 2). From January to April, no clear patterns for the correlations of radial growth and precipitation were observed (Fig. 3). In comparison, radial growth often showed strong positive responses to precipitation of current May and June (Fig. 3). Incidentally, the responses of radial growth to CMI were very similar to precipitation (Appendix S3).

3.2.2 Linear mixed model

For all 40 sites, precipitation of both previous and current growing season often had a positive effect on the radial growth (Table 2), which was consistent with climate moisture index (see Appendix S4). The temperature of previous summer negatively influences the growth of white spruce, then became positive in winter, followed by negative and positive effect in March and April, respectively (Table 2). In the following season, the effect of temperature on the growth of tree-ring width turned to negative in June again (Table 2). In contrast to the strong negative effects of temperature of previous summer, the growth of white spruce was positively influenced by the temperature of current July (Table 2).

Table 2. Estimates of the linear mixed models for the effect of monthly total precipitation (P), monthly mean temperature (T_{mean}) of previous year (from May to Dec) and current year (from Jan to Aug) on the tree-ring width of white spruce. “ns”, one asterisk and two asterisks represent $p \geq 0.05$, $p<0.05$ and $p<0.01$, respectively.

Variables	Previous year	Estimate	SE	*t* value	Sig.	Current year	Estimate	SE	*t* value	Sig.
P	May	0.081	0.022	3.748	**	Jan	0.018	0.026	0.719	ns
	June	0.032	0.023	1.414	ns	Feb	0.023	0.022	1.046	ns
	July	0.087	0.022	4.024	**	Mar	-0.002	0.022	-0.100	ns
	Aug	0.173	0.022	7.812	**	Apr	-0.017	0.022	-0.774	ns
	Sep	0.044	0.022	2.024	*	May	0.150	0.026	5.740	**
	Oct	-0.028	0.024	-1.161	ns	Jun	0.135	0.022	6.011	**
	Nov	0.023	0.024	0.956	ns	Jul	0.061	0.022	2.846	**
	Dec	-0.001	0.022	-0.032	ns	Aug	0.041	0.022	1.885	ns
T_{mean}	May	-0.090	0.023	-3.871	**	Jan	0.060	0.022	2.800	**
	June	-0.005	0.022	-0.248	ns	Feb	-0.006	0.022	-0.298	ns
	July	-0.049	0.022	-2.240	*	Mar	-0.042	0.022	-1.970	*
	Aug	-0.172	0.022	-7.840	**	Apr	0.050	0.022	2.342	*
	Sep	-0.048	0.022	-2.118	*	May	0.021	0.022	0.955	ns
	Oct	0.055	0.022	2.522	*	Jun	-0.049	0.022	-2.265	*
	Nov	0.003	0.022	0.153	ns	Jul	0.078	0.021	3.622	**
	Dec	0.063	0.022	2.911	**	Aug	0.037	0.022	1.735	ns

3.2.3 VS-Lite model

A correlation analysis between the VS-Lite estimated chronologies and the true chronologies found that 30 out of 40 sites were significantly correlated (mean r=0.33, SD=0.11) (Appendix S5). The simulated values of the temperature-induced growth g_T was generally zero in cold winter, followed by a gradually increasing and peaked in summer (Fig. 4). The soil moisture-related growth curve g_M was affected by both precipitation and temperature. The pointwise minimum of the simulated g_T and g_M

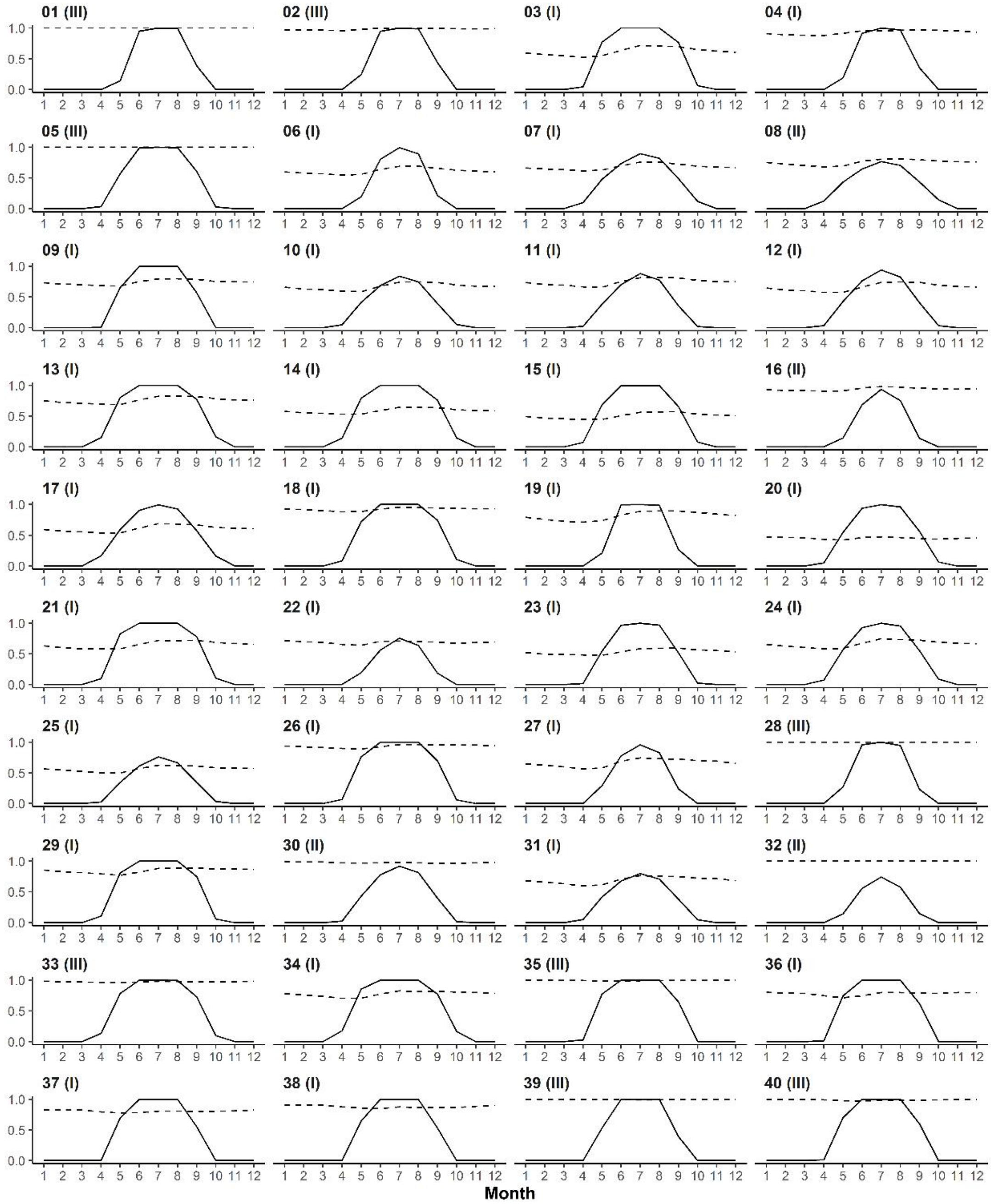

Fig. 4 Simulated growth response curves of temperature and soil moistures. The solid and dashed lines represent the response curves of temperature and soil moisture, respectively. The labels I (moisture limited), II (temperature limited) and III (neither limited by temperature nor moisture) show the growth pattern of each site.

curves determines which variable is limiting in any given month. According to the modeled temperature and soil moisture growth response curves g_T and g_M (Fig. 4), the forty radial growth patterns can be divided into three groups: pattern I, moisture limited; pattern II, temperature limited; and pattern III, neither limited by temperature nor moisture. The correlations of the averaged observed and simulated chronologies for the three patterns were all significant, which were 0.465, 0.296, and 0.566, respectively (Appendix S6). For example, the radial growth in sites 3 and 6 was mainly limited by moisture while it was limited by temperature for the radial growth in site 8 (Fig. 4). In comparison, the simulated values of g_T and g_M, from June to August, were similar for the radial growth in sites 1, 2 and 5, and were therefore classified as pattern III (Fig. 4). In total, the radial growth in 28 sites was limited by moisture while the temperature limited ones were only found in four sites (site 08, 16, 30, 32; Fig. 4). There were eight sites where the pattern III was found due to similar simulated values of g_T and g_M in summer (Fig. 4). The results indicated that the growth of white spruce was most often limited by soil moisture as opposed to temperature and varied spatially.

3.3 Difference of the growth-climate relationship along different elevations, latitudes, and growing degree days (GDD > 5℃)

The results of VS-Lite model showed, in total, the radial growth in 28 sites was limited by soil moisture, which distributed extensively from 53.05° N to 58.53° (Fig. 4, Appendix S2). The four sites with pattern II located from 54.48° N to 57.15° N. In comparison, the pattern III was found in these sites along two limited latitude: 52.05° N to 53.75° N, and 57.85° N to 58.78° N (Fig. 4, Appendix S2).

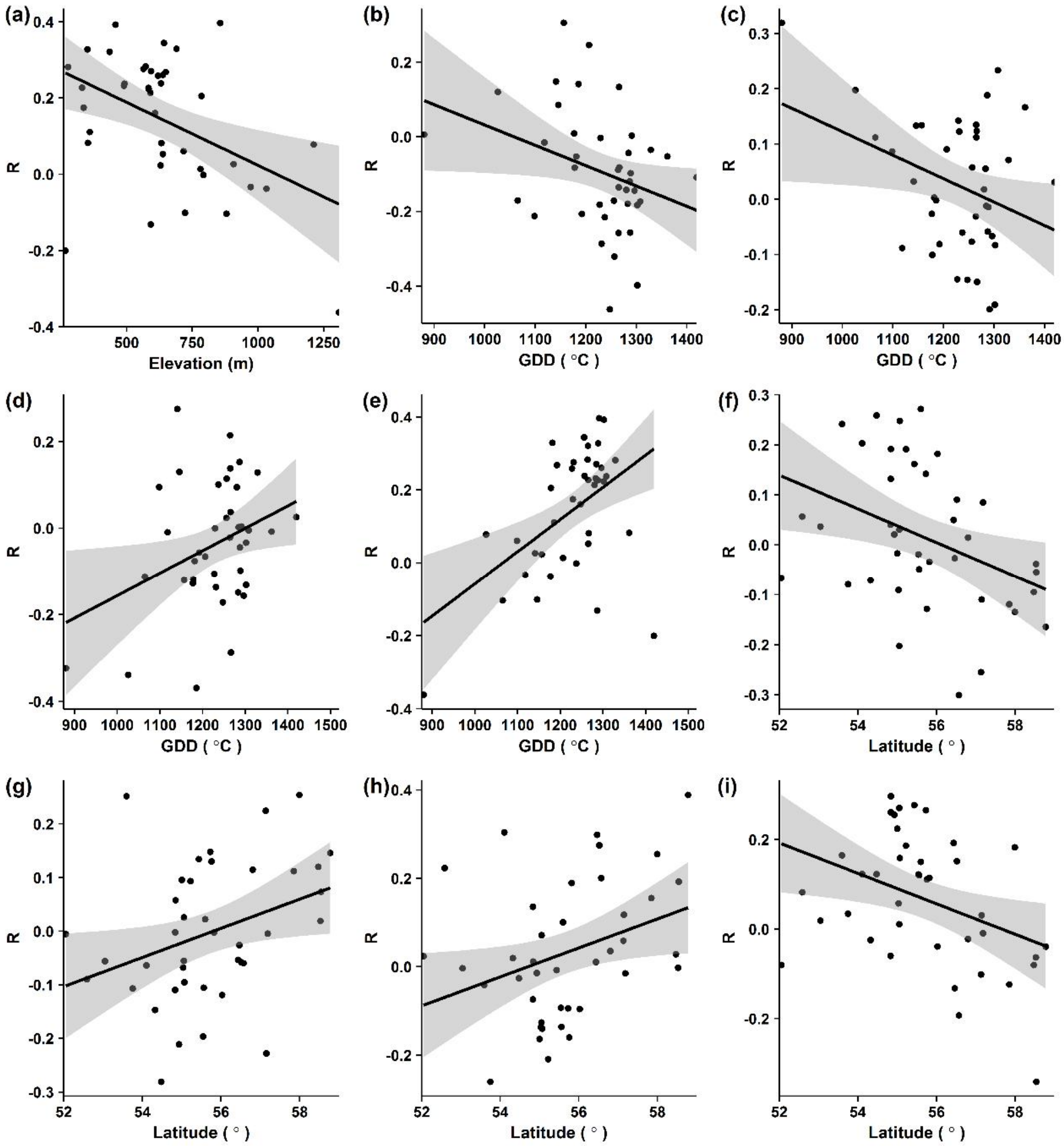

Fig. 5 Variations in the correlations of radial growth and (a) monthly total precipitation of current May with elevation; (b) monthly mean temperature of previous May with growing degree days (GDD > 5℃) , (c) monthly mean temperature of current May with growing degree days (GDD > 5℃) , (d) monthly total precipitation of previous October with growing degree days (GDD > 5°C), (e) monthly total

precipitation of current May with growing degree days (GDD > 5℃); (f) monthly mean temperature of previous June with different latitudes, (g) monthly mean temperature of previous November with different latitudes, (h) monthly total precipitation of previous June with different latitudes, (i) monthly total precipitation of current July with different latitudes. The shaded area presents 95% confidence intervals.

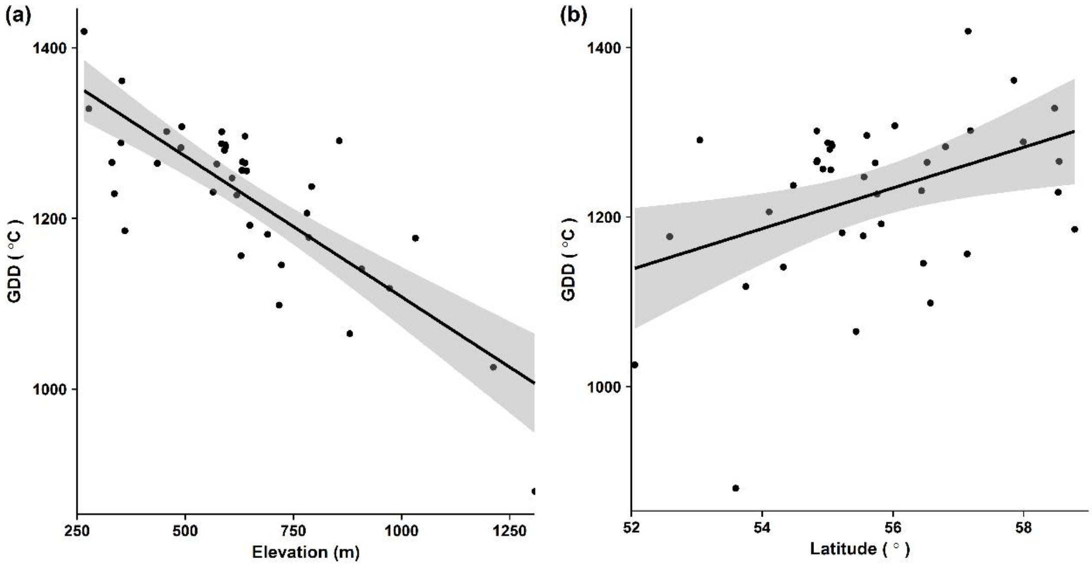

Fig. 6 Variation of growing degree days (GDD > 5℃) with (a) elevations, and (b) latitudes. The shaded area presents 95% confidence intervals.

The correlation coefficients of radial growth and monthly total precipitation of current May decreased with increasing elevation (Fig. 5a, p=0.038). Similarly, correlations of radial growth and monthly mean temperature of previous May (Fig. 5b, p=0.041) and current May (Fig. 5c, p=0.034) decreased with increasing GDD. In comparison, correlations of radial growth and monthly total precipitation of previous October (Fig. 5d, *p*=0.029) and current May (Fig. 5e, *p*=0.001) increased with GDD. The correlations of radial growth and monthly mean temperature of previous June (Fig. 5f, *p*=0.016), and monthly total precipitation of current July (Fig. 5i, *p*=0.016) declined when latitudes increased. In contrast, as latitudes increased, correlations of radial growth and monthly mean temperature of previous November (Fig. 5g, *p*=0.031), and monthly total precipitation of previous June (Fig. 5h, *p*=0.031) increased. In the study area, GDD decreased with increasing elevations while it increased with increasing latitudes (Fig. 6). In summary, the correlations of radial growth and temperature decreased with increasing GDD while the correlations of radial growth and precipitation showed an upward trend when the GDD increased (Fig. 5). It suggests that the radial growth of white spruce in northern stands is often more strongly limited by temperature-induced drought due to the higher GDD.

4. Discussion

Growth estimates from the nonlinear process-based VS-Lite model indicated that soil moisture often limited the radial growth of white spruce at most sites and temperature-induced drought was the primary limiting factor for radial growth. In addition, the radial growth of white spruce in northern stands is often more strongly limited by temperature-induced drought due to the higher temperature and lower precipitation in growing season. As the global climate change is in progress, specific forest management strategies that mitigate the potential effects of increased drought stress are needed to maintain these forests.

4.1 Response of radial growth to climate variables

The correlation analysis indicated that the previous year summer temperature imposed a strong negative impact on the radial growth of white spruce while the precipitation of previous year had significant and positive impacts on the radial growth (Fig. 2). In summer, the high temperature can increase evapotranspiration, resulting in water deficit (D'Arrigo et al., 2004; Huang et al., 2010), which was also confirmed by the results of our VS-Lite model. The impact of previous year temperature was also consistent with the carry-over effect (Cook and Kairiukstis, 1990; Fritts, 2001; Rammig et al., 2015), which refers to the phenomenon that nutrient storage of the previous year also exerts significant effect on the growth of the following year. Likewise, the total photosynthates of previous year could be reduced owing to the temperature-induced drought. As a result, the growth rate of white spruce in the following year declined due to the insufficient carbohydrates stored.

In current growing season, radial growth was often positively correlated with precipitation of current May and June while showed a negative response to the temperature (Fig. 3). In a water-deficit environment, sufficient precipitation can promptly alleviate the drought stress and impose a positive effect on radial growth through improving the production of total xylem cell (Deslauriers et al., 2016).

Therefore, the strong positive effect of precipitation on the radial growth was observed in both previous and current growing season. Overall, these results suggest that drought is the primary limiting factor for the growth of white spruce. Prior to the onset of winter freezing, white spruce could perform photosynthesis to store energy and impose a positive effect on the radial growth like other evergreen conifers (Malhi et al., 1999; Miyazawa and Kikuzawa, 2005). As a consequence, the radial growth positively correlated with temperature between October and December of the previous year (Table 2, Fig. 2).

4.2 Assessment of the VS-Lite model

The results of the VS-Lite model indicated that the radial growth in 28 sites were limited by moisture while the temperature limited ones were only found in four sites (Fig. 4). With these results, the VS-Lite model also revealed that temperature-induced drought was the main limiting factor for the radial growth of white spruce. Compared with the empirical linear statistics, the model can directly reflect the impact of soil moisture. For example, the correlation analysis can only reflect the indirect impact of temperature and precipitation on the radial growth, then inferring the temperature-induced drought effect. In addition, the model can describe the monthly variation in the response of radial growth to climate variables through the simulated response curves of g_T and g_M (Fig. 4). In summary, the VS-Lite model can capture the drought signal and simulate the radial growth of white spruce in the boreal forest of Alberta. For example, according to the results of VS-Lite model, there were eight sites where the simulated values of

g_T and g_M in summer were similar (Fig. 5). It suggests that the radial growth in these sites was limited neither by temperature nor precipitation, which might be contributed by the site-specific effects (Gewehr et al., 2014). However, 10 out of 40 simulated tree-ring chronologies did not significantly correlate with the actual residual chronologies (*p*>0.05). This suggests that improvement is still needed for the VS-Lite model to more accurately simulate the responses of radial growth to climate variables and predict the impact of climate change on forest ecosystems. Other factors such as competition or micro-site conditions (Huang et al., 2013) might play an important role in determining the tree growth at these mid-latitude boreal sites, and have the potential to be included in future versions of the model.

4.3 Spatial variations in the growth-climate relationship

Results indicated that the radial growth in northern sites is more likely to suffer from drought stress (Fig. 5). Overall, typical dry continental climate with cold winters and warm summers prevail in the study area (Canada, 2010). During the period between 1971 and 2000, at the southern part of the study area, the mean annual total precipitation was 535.4 mm with 30% in the form of snow and in the northern area, the value was 394.1 mm (34% as snow) (Canada, 2010). Therefore, mean annual precipitation in the higher latitudes was ca. 140 mm less than in lower latitudes, and the percentage of precipitation in the form of snow in higher latitudes exceeds that of in lower latitudes. Consequently, the radial growth of white spruce in northern stands is more strongly limited by temperature-induced drought due to the higher GDD and lower precipitation.

Results showed that the correlations of radial growth and monthly total precipitation in current July decreased with the increasing of latitudes (Fig. 5i), which was opposite to the latitudinal response for the precipitation in previous June (Fig. 5h). In a water-deficit environment, an increment of precipitation can promptly alleviate the drought stress and promote radial growth (Deslauriers et al., 2016). In the study region, the monthly total precipitation and monthly mean temperature often increased from June to July (Appendix S7). However, more precipitation dropped in northern region than the southern region (Appendix S8a). In contrast, less temperature increased in the northern region than the southern region (Appendix S8b). As a result, in July, trees in the south often grow in a hot and dry environment, therefore radial growth being more sensitive and positively responding to the increment of precipitation in the south.

In winter, with the increasing of latitudes, correlations of radial growth and temperature of previous November gradually converted from negative to positive (Fig. 5g). The Chinook winds that occurred in southern Alberta can reduce tree growth through drastically raising the winter temperature and contributing to the loss of soil moisture (Lotan and Critchfield, 1990; Nkemdirim, 1996; Chhin et al., 2008). As a consequence, the latitudinal response to the temperature-growth relationship in winter was negative in southern regions. In comparison, at low winter temperature in higher latitudes, due to freezing stress a warmer winter could reduce the damage of tree tissues, such as buds and roots (Miller-Rushing and Primack, 2008). In addition, in early winter with higher temperature, white spruce could perform photosynthesis to store energy and impose a positive effect on the radial growth like other evergreen coniferous species (Malhi et al., 1999; Miyazawa and Kikuzawa, 2005). At last, the initiation of growth could also be delayed for freezing-induced cavitation in cold winter (Wang et al., 1992). Therefore, a warmer early winter is able to facilitate the growth of white spruce in northern area.

5. Conclusions

Temperature-induced drought was the dominant limiting factor for the radial growth of white spruce, which contributed to the spatial variation in climate-growth relationship as well. The rate of warming in the Canadian boreal forests is predicted to be twice the global average, which will likely lead to severe drought stress in Alberta boreal forests over the next several decades (Price et al., 2013; Wang et al., 2014). To maintain and utilize these forests sustainably, considerable concern on the temperature-induced drought issue is needed in the future forest management. In addition, for the potential nonlinear and unstable response of white spruce to climate variables, process-based forward models in combination with climate predictions from global circulation models have the potential to predict future outcomes from these forests.

Acknowledgements

This project was funded by the 100 Talents Program of the Chinese Academy of Sciences [CAS project number Y421081001]. National Natural Science Foundation of China [NSFC grant numbers 31550110208, 31570584], China Postdoctoral Science

Foundation [grant number 2015M582433], Academy of Finland [projects numbers 1284701, 1282842, 285630] and ICOS-Finland [project number 281255]. LC thanks the China Scholarship Council (CSC) for supporting his studies in Japan. Other funding agencies include National Natural Science Foundation of China [grant number 31570584], Natural Science and Engineering Research Council of Canada, Mixedwood Management Association, and Forest Resource Improvement Association of Alberta.

References

Andreu-Hayles, L., D'arrigo, R., Anchukaitis, K.J., Beck, P.S., Frank. D., Goetz, S., 2011. Varying boreal forest response to Arctic environmental change at the Firth River, Alaska. Environ. Res. Lett., 6(4), 045503, doi:10.1088/1748-9326/6/4/045503.

AESRD, 2012. Phase 3 Forest Inventory. Alberta Environment and Sustainable Resource Development, Available from: http://srd.alberta.ca/ MapsPhotosPublications/Maps/ResourceData Product Catalogue/ ForestVegetationInventories.aspx [Access on July 8, 2013].

Bates, D., Maechler, M., Bolker, B., Walker, S., 2014. LME4: Linear mixed-effects models using Eigen and S4. R package version, 1.

Beckingham, J., Corns, I., Archibald, J., 1996. Field Guide to Ecosites of West-central Alberta. Natural Resources Canada. Canadian Forest Service, northwest Region, northern Forestry Centre Special Report, 9.

Breitenmoser, P., Brönnimann, S., Frank, D., 2014. Forward modelling of tree-ring width and comparison with a global network of tree-ring chronologies. Clim. Past, 10(2), 437−449.

Bunn, A.G., 2008. A dendrochronology program library in R (dplR). Dendrochronologia, 26(2), 115−124.

Canada, E., 2010. Canadian Climate Normals or Averages 1971-2000. National

Climate Data and Information Archive.

Chhin, S., Hogg, E.T., Lieffers, V.J. and Huang, S., 2008. Potential effects of climate change on the growth of lodgepole pine across diameter size classes and ecological regions. For. Ecol. Manage., 256(10): 1692-1703.

Chavardès, R.D., Daniels, L.D., Waeber, P.O., Innes, J.L., Nitschke, C.R., 2013 Unstable climate− growth relations for white spruce in southwest Yukon, Canada. Clim. change, 116(3−4), 593−611.

Cook, E.R., Esper, J., D’Arrigo, R.D., 2004. Extra-tropical Northern Hemisphere land temperature variability over the past 1000 years. Quat. Sci. Rev., 23(20), 2063−2074.

Cook, E.R., Kairiukstis, L.A., 1990. Methods of dendrochronology: applications in the environmental sciences, Kluwer, Dordrecht.

Cumming, S., Schmiegelow, F., Burton, P., 2000. Gap dynamics in boreal aspen stands: is the forest older than we think? Ecol. Appl., 10(3), 744−759.

D'Arrigo, R., Wilson, R. and Jacoby, G., 2006. On the long-term context for late twentieth century warming. On the long-term context for late twentieth century warming. J. Geophys. Res., 111, D03103, doi:10.1029/2005JD006352.

D'Arrigo, R., Wilson, R., Liepert, B., Cherubini, P., 2008. On the ‘divergence problem’ in northern forests: a review of the tree-ring evidence and possible causes. Global Planet. Change, 60(3), 289−305.

D'arrigo, R.D., Kaufmann, R.K., Davi, N., Jacoby, G.C., Laskowski, C., Myneni, R.B., Cherubini, P., 2004. Thresholds for warming-induced growth decline at elevational tree line in the Yukon Territory, Canada. Global Biogeochem. Cycles, 18(3).

Deslauriers, A., Huang, J.-G., Balducci, L., Beaulieu, M., Rossi, S., 2016. The contribution of carbon and water in modulating wood formation in black spruce saplings. Plant Physiol., 170(4), 2072−2084.

Dixon, R.K., Solomon, A., Brown, S., Houghton, R., Trexier, M., Wisniewski, J., 1994. Carbon pools and flux of global forest ecosystems. Science, 263, 185−190.

Esper, J., Cook, E.R., Schweingruber, F.H., 2002. Low-frequency signals in long tree-ring chronologies for reconstructing past temperature variability. Science, 295(5563), 2250−2253.

Esper, J., Frank, D., 2009. Divergence pitfalls in tree-ring research. Clim. Change, 94(3), 261−266.

Fritts, H., 2001. Tree Rings and Climate. The Blackburn Press, Caldwell.

Gewehr, S., Drobyshev, I., Berninger, F. and Bergeron, Y., 2014. Soil characteristics mediate the distribution and response of boreal trees to climatic variability. Can. J. For. Res., 44(5): 487-498.

Hogg, E., Barr, A., Black, T., 2013. A simple soil moisture index for representing multi-year drought impacts on aspen productivity in the western Canadian interior. Agric. For. Meteorol., 178, 173−182.

Hogg, E., Brandt, J., Michaelian, M., 2008. Impacts of a regional drought on the productivity, dieback, and biomass of western Canadian aspen forests. Can. J. For. Res., 38(6), 1373−1384.

Hogg, E., Brandt, J.P., Kochtubajda, B., 2005. Factors affecting interannual variation in growth of western Canadian aspen forests during 1951-2000. Can. J. For. Res., 35(3), 610−622.

Hogg, E.H., 1994. Climate and the southern limit of the western Canadian boreal forest. Can. J. For. Res., 24(9), 1835−1845.

Hogg, E.H., 1997. Temporal scaling of moisture and the forest-grassland boundary in western Canada. Agric. For. Meteorol., 84(1), 115−122.

Holmes, R.L., 1983. Computer-assisted quality control in tree-ring dating and measurement. Tree-Ring Bull., 43, 69–78.

Huang, J.-G., Stadt, K.J., Dawson, A., Comeau, P.G., 2013. Modelling growth-competition relationships in trembling aspen and white spruce mixed boreal forests of Western Canada. PLoS One, 8(10): e77607, doi:10.1371/journal.pone.0077607.

Huang, J., Tardif, J.C., Bergeron, Y., Denneler, B., Berninger, F., Girardin, M.P., 2010.

Radial growth response of four dominant boreal tree species to climate along a latitudinal gradient in the eastern Canadian boreal forest. Glob. Change Biol., 16, 711–731.

Hughes, M.K., Swetnam, T.W., Diaz, H.F. 2010. Dendroclimatology: progress and prospects, Springer Science & Business Media.

Hutchinson, M.F., 2004. ANUSPLIN Version 4.3. Center for Resource and Environmental Studies, Australian National University, Available at http://fennerschool.anu.edu.au/publications /software/ anusplin.php [accessed 12 December 2008].

Intergovernmental Panel on Climate Change (IPCC), 2014. ‘Agriculture, forestry, and other land use.’ Chapter 11 in Climate Change 2014: Mitigation of Climate Change. Available at: https://www.ipcc.ch/report/ar5/wg3/ (accessed 15 August 2014).

Jacoby, G.C., D'Arrigo, R.D., 1995. Tree ring width and density evidence of climatic and potential forest change in Alaska. Global Biogeochem. Cycles, 9(2), 227–234.

Jones, P.D., Briffa, K.R., Osborn, T.J., Lough, J.M., Van Ommen, T.D., Vinther, B.M., ... & Xoplaki, E., 2009. High-resolution palaeoclimatology of the last millennium: a review of current status and future prospects. The Holocene, 19(1), 3–49.

Kasischke, E.S., Stocks, B.J., 2012. Fire, climate change, and carbon cycling in the boreal forest, 138. Springer Science & Business Media.

Lindahl, B.D., Ihrmark, K., Boberg, J., Trumbore, S.E., Högberg, P., Stenlid, J., Finlay, R.D., 2007. Spatial separation of litter decomposition and mycorrhizal nitrogen uptake in a boreal forest. New Phytol., 173(3), 611–620.

Lotan, J.E. and Critchfield, W.B., 1990. Pinus contorta Dougl. ex. Loud. Silvics of North America, 1: 302-315.

Lloyd, A.H., Bunn, A.G., Berner, L., 2011. A latitudinal gradient in tree growth response to climate warming in the Siberian taiga. Global Change Biol., 17(5), 1935–1945.

Lloyd, A.H., Duffy, P.A., Mann, D.H., 2013. Nonlinear responses of white spruce growth to climate variability in interior Alaska. Can. J. For. Res., 43(999), 331–343.

Lloyd, A.H., Fastie, C.L., 2002. Spatial and temporal variability in the growth and climate response of treeline trees in Alaska. Clim. Change, 52(4), 481–509.

Mäkinen, H., Nöjd, P., Kahle, H.P., Neumann, U., Tveite, B., Mielikäinen, K., Röhle, H. and Spiecker, H., 2002. Radial growth variation of Norway spruce (*Picea abies* (L.) Karst.) across latitudinal and altitudinal gradients in central and northern Europe. For. Ecol. Manage., 171(3), 243–259.

Malhi, Y., Baldocchi, D., Jarvis, P., 1999. The carbon balance of tropical, temperate and boreal forests. Plant Cell Environ., 22(6), 715–740.

Mann, M.E., Bradley, R.S., Hughes, M.K., 2002. Northern Hemisphere temperatures during the past millennium: inferences, uncertainties, and limitations. Geophys. Res. Lett., 26(6), 759–762.

Ma, Z., Peng, C., Zhu, Q., Chen, H., Yu, G., Li, W., Zhou, X., Wang, W., Zhang, W., 2012. Regional drought-induced reduction in the biomass carbon sink of Canada's boreal forests. Proc. Natl. Acad. Sci. U.S.A., 109(7):2423-2427.

Michaelian, M., Hogg, E.H., Hall, R.J., Arsenault, E., 2011. Massive mortality of aspen following severe drought along the southern edge of the Canadian boreal forest. Global Change Biol., 17(6), 2084–2094.

Miller-Rushing, A.J., Primack, R.B., 2008. Effects of winter temperatures on two birch (Betula) species. Tree Physiol., 28(4), 659–664.

Miyazawa, Y., Kikuzawa, K., 2005. Winter photosynthesis by saplings of evergreen broad-leaved trees in a deciduous temperate forest. New Phytol., 165(3), 857–866.

Nkemdirim, L.C., 1996. Canada's chinook belt. Int. J. climatol., 16(4): 441-462.

Peng, C. et al., 2011. A drought-induced pervasive increase in tree mortality across Canada's boreal forests. Nat. Clim. Change, 1(9): 467-471.

Porter, T.J., Pisaric, M.F., 2011. Temperature-growth divergence in white spruce forests of Old Crow Flats, Yukon Territory, and adjacent regions of northwestern North America. Global Change Biol., 17(11), 3418–3430.

Price, D.T., Alfaro, R.I., Brown, K.J., Flannigan, M.D., Fleming, R.A., Hogg, E.H., Girardin, M.P., Lakusta, T., Johnston, M., McKenney, D.W., Pedlar, J.H., 2013. Anticipating the consequences of climate change for Canada’s boreal forest ecosystems. Environ. Rev., 21(4), 322–365.

Rammig, A., Wiedermann, M., Donges, J.F., Babst, F., von Bloh, W., Frank, D., Thonicke, K. and Mahecha, M.D., 2015. Coincidences of climate extremes and anomalous vegetation responses: comparing tree ring patterns to simulated productivity. Biogeosciences, 12(2), 373–385.

Speer, J.H., 2010. Fundamentals of tree-ring research, University of Arizona Press.

Stadt, K.J., Huston, C., Coates, K.D., Feng, Z., Dale, M.R., Lieffers, V.J., 2007. Evaluation of competition and light estimation indices for predicting diameter growth in mature boreal mixed forests. Ann. For. Sci., 64(5), 477–490.

Stocks, B.J., Fosberg, M.A., Lynham, T.J., Mearns, L., Wotton, B.M., Yang, Q., Jin, J.Z., Lawrence, K., Hartley, G.R., Mason, J.A. and McKenney, D.W., 1998. Climate change and forest fire potential in Russian and Canadian boreal forests. Clim. Change, 38(1), 1–13.

R Core Team, 2015. R: A language and environment for statistical computing. R Foundation for Statistical Computing, Vienna, Austria. URL https://www.R-project.org/.

Tolwinski-Ward, S., Anchukaitis, K.J., Evans, M.N., 2013. Bayesian parameter estimation and interpretation for an intermediate model of tree-ring width. Clim. Past, 9, 1481–1493.

Tolwinski-Ward, S.E., Evans, M.N., Hughes, M.K., Anchukaitis, K.J., 2011. An efficient forward model of the climate controls on interannual variation in tree-ring width. Clim. Dyn., 36(11-12), 2419–2439.

Touchan, R., Shishov, V., Meko, D., Nouiri, I., Grachev, A., 2012. Process based model sheds light on climate sensitivity of Mediterranean tree-ring width.

Biogeosciences, 9(3), 965–972.

Vaganov, E.A., Anchukaitis, K.J., Evans, M.N., 2011. How well understood are the processes that create dendroclimatic records? A mechanistic model of the climatic control on conifer tree-ring growth dynamics. In Dendroclimatology. Springer Science & Business Media.

Vaganov, E.A., Hughes, M.K., Shashkin, A.V., 2006. Growth dynamics of conifer tree rings: images of past and future environments. Springer Science & Business Media.

Visser, H., Büntgen, U., D'Arrigo, R., Petersen, A., 2010. Detecting instabilities in tree-ring proxy calibration. Clim. Past, 6(3), 367–377.

Volney, W.J.A., Fleming, R.A., 2000. Climate change and impacts of boreal forest insects. Agric., Ecosyst. Environ., 82(1), 283–294.

Wang, J., Ives, N., Lechowicz, M., 1992. The relation of foliar phenology to xylem embolism in trees. Funct. Ecol., 6(4), 469–475.

Wang, Y., Hogg, E.H., Price, D.T., Edwards, J., Williamson, T., 2014. Past and projected future changes in moisture conditions in the Canadian boreal forest. The Forestry Chronicle, 90(5), 678–691.

Wilmking, M., Juday, G.P., Barber, V.A., Zald, H.S., 2004. Recent climate warming forces contrasting growth responses of white spruce at tree line in Alaska through temperature thresholds. Global Change Biol., 10(10), 1724–1736.

Zhang, Y., Shao, X., Xu, Y., Wilmking, M., 2011. Process-based modeling analyses of Sabina przewalskii growth response to climate factors around the northeastern Qaidam Basin. Chin. Sci. Bull., 56(14), 1518–1525.

Zhang, Y. and Wilmking, M., 2010. Divergent growth responses and increasing temperature limitation of Qinghai spruce growth along an elevation gradient at the northeast Tibet Plateau. For. Ecol. Manage., 260(6), 1076–1082.

Supporting Information

Appendix S1. Information of annual total precipitation, minimum temperature ($T_{\min}$), mean temperature (T_{mean}) and maximum temperature ($T_{\max}$) from 1930 to 2010 for the 40 white spruce sites along different latitudes.

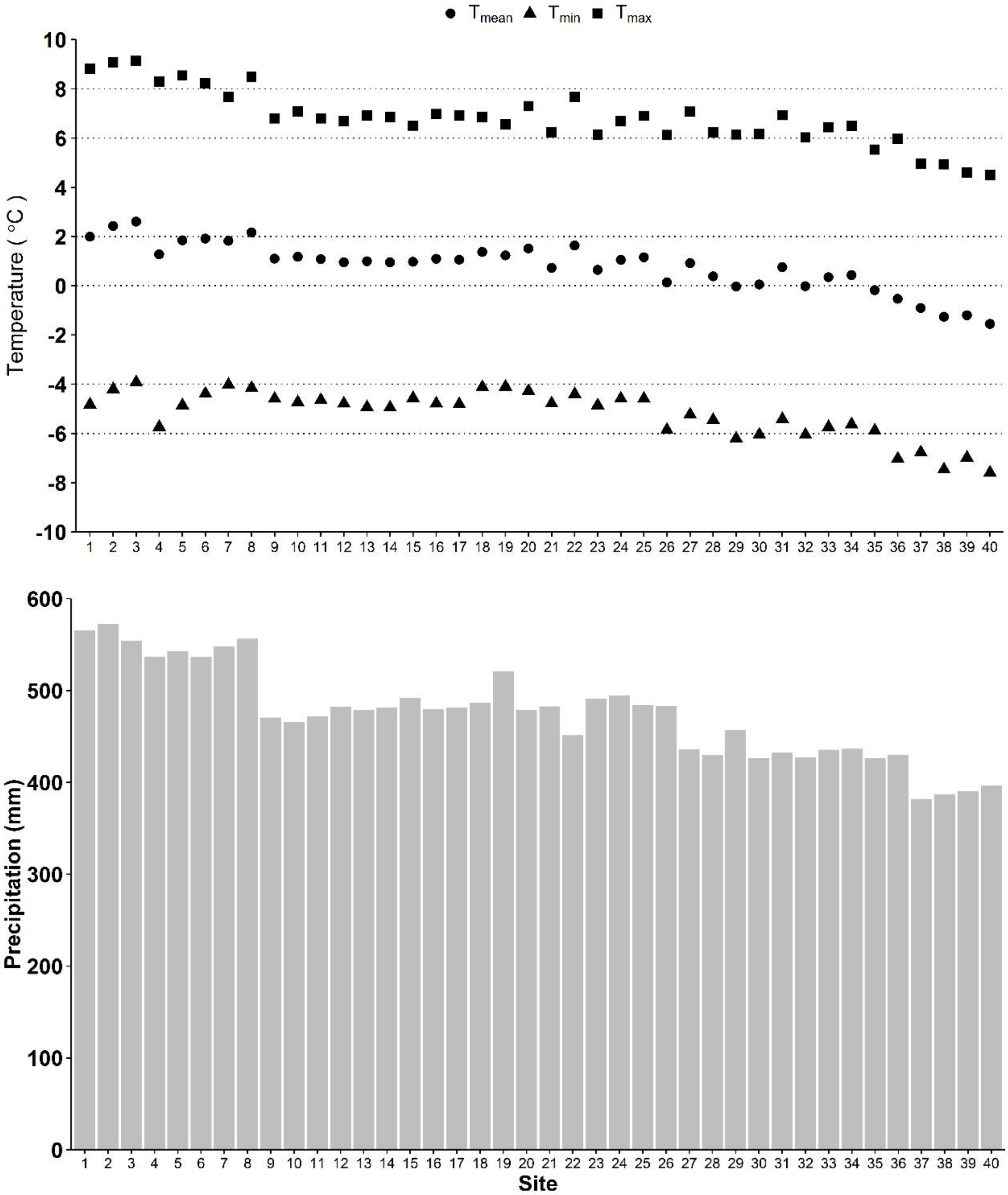

Appendix S2. Statistical information of the standard chronologies of white spruce.

Site	Latitude	Longitude	Elevation (m)	First year	Last year	Span (yrs.)	Tree-ring width (mm)		Skew	AR1
							Mean	SD		
S01	52.049	-115.078	1212	1967	2010	44	1.487	0.806	-0.553	0.11
S02	52.584	-115.353	1032	1975	2010	36	0.794	0.364	-0.73	-0.084
S03	53.045	-115.014	856	1964	2010	47	1.330	0.936	0.261	0.503
S04	53.595	-117.669	1308	1980	2007	28	1.196	1.202	-0.144	-0.145
S05	53.75	-116.618	972	1967	2010	44	1.171	0.574	0.947	0.104
S06	54.104	-115.746	781	1949	2010	62	1.098	0.790	0.534	0.402
S07	54.322	-115.704	907	1950	2010	61	1.103	0.825	0.058	0.076
S08	54.476	-116.789	792	1953	2010	58	1.105	0.793	0.098	0.475
S09	54.831	-111.713	638	1930	2010	81	1.031	0.801	1.593	0.547
S10	54.834	-111.838	584	1954	2010	57	1.241	0.724	0.248	0.076
S11	54.841	-111.683	632	1955	2010	56	1.359	0.711	-0.598	0.374
S12	54.929	-111.543	631	1955	2010	56	1.281	0.763	-0.276	0.157
S13	55.002	-111.726	583	1953	2010	58	1.231	0.985	-0.026	0.476
S14	55.034	-111.681	590	1957	2010	54	1.553	0.839	2.157	0.241
S15	55.052	-111.271	642	1947	2010	64	1.247	0.657	-0.422	0.478
S16	55.055	-111.904	592	1961	2010	50	1.478	0.792	0.258	0.143
S17	55.067	-111.811	593	1960	2010	51	1.824	0.954	0.611	-0.058
S18	55.223	-114.523	690	1943	2010	68	1.579	1.093	0.118	0.704
S19	55.436	-114.501	880	1978	2010	33	3.080	1.353	-0.72	0.121
S20	55.544	-118.742	785	1956	2010	55	1.552	0.976	1.115	0.365
S21	55.558	-111.237	608	1954	2010	57	1.777	0.961	-0.5	0.183
S22	55.599	-118.109	638	1956	2010	55	1.635	1.019	-0.089	0.111
S23	55.728	-110.982	573	1953	2010	58	0.701	0.452	-0.064	0.469
S24	55.757	-114.177	619	1953	2010	58	1.349	0.908	0.304	0.482
S25	55.82	-115.212	649	1945	2010	66	0.593	0.421	-0.092	0.571
S26	56.026	-110.883	492	1957	2010	54	1.033	0.686	0.184	0.376
S27	56.436	-115.325	564	1965	2010	46	0.796	0.792	-0.909	0.009
S28	56.465	-118.313	722	1968	2010	43	1.170	0.954	-1.1	0.284
S29	56.519	-111.298	435	1967	2010	44	0.955	0.544	-0.322	0.27
S30	56.571	-118.747	717	1954	2010	57	0.921	0.715	-0.259	0.407
S31	56.803	-115.258	490	1953	2010	58	0.728	0.650	0.126	0.249
S32	57.136	-117.73	629	1974	2010	37	1.393	0.950	-0.476	0.466
S33	57.15	-111.638	266	1963	2010	48	0.885	0.574	-0.403	0.45
S34	57.187	-115.115	457	1952	2010	59	0.709	0.622	-0.035	0.371
S35	57.85	-115.376	353	1952	2010	59	0.900	0.627	-0.482	0.353
S36	57.994	-117.417	351	1956	2010	55	0.891	0.447	0.059	0.17
S37	58.473	-115.787	277	1937	2010	74	0.772	0.633	-0.068	0.617
S38	58.529	-117.292	336	1936	2010	75	0.982	0.666	-0.284	0.658
S39	58.542	-115.616	330	1956	2010	55	1.021	0.561	0.396	0.503
S40	58.781	-117.378	360	1949	2010	62	0.515	0.394	0.558	0.553

Appendix S3. Bootstrapped correlation coefficients of radial growth and climate moisture index of (a) previous year and (b) current year. One asterisk and two asterisks represent $p<0.05$, $p<0.01$, respectively.

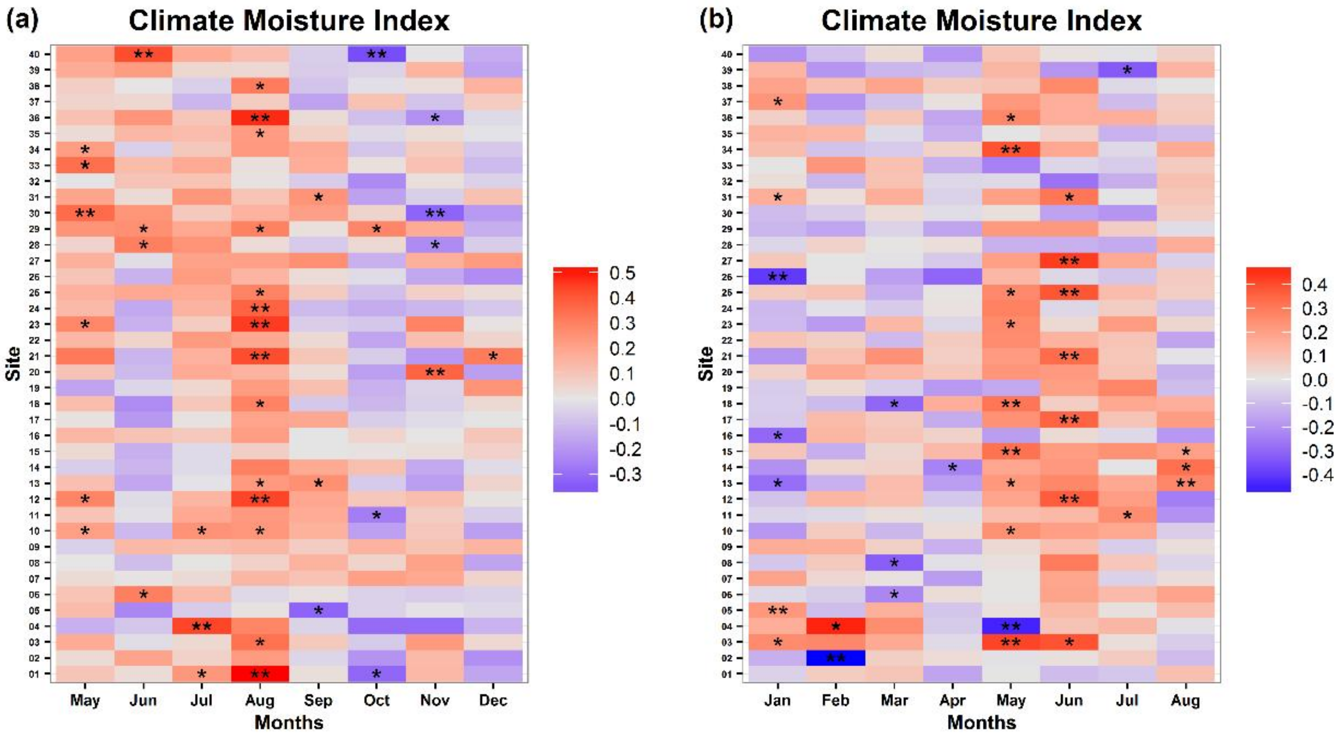

Appendix S4. Estimates of the linear mixed models for the effect of climate moisture index (CMI) on the tree-ring width of white spruce. “ns”, one asterisk and two asterisks represent $p \geq 0.05$, $p < 0.05$ and $p < 0.01$, respectively.

Month	Estimate	SE	*t* value	Sig.	Month	Estimate	SE	*t* value	Sig.
May	0.106	0.022	4.916	**	Jan	0.019	0.026	0.732	ns
June	0.030	0.024	1.262	ns	Feb	0.016	0.022	0.753	ns
July	0.094	0.022	4.353	**	Mar	0.013	0.022	0.612	ns
Aug	0.200	0.022	9.084	**	Apr	-0.040	0.022	-1.835	ns
Sep	0.056	0.022	2.564	*	May	0.126	0.025	5.008	**
Oct	-0.048	0.023	-2.04	*	Jun	0.147	0.023	6.326	**
Nov	0.025	0.024	1.043	ns	Jul	0.043	0.022	1.975	*
Dec	-0.001	0.022	-0.041	ns	Aug	0.038	0.022	1.773	ns

Appendix S5. Correlations between the actual and simulated residual chronologies using VS-Lite model. One asterisk and two asterisks represent $p<0.05$, $p<0.01$, respectively.

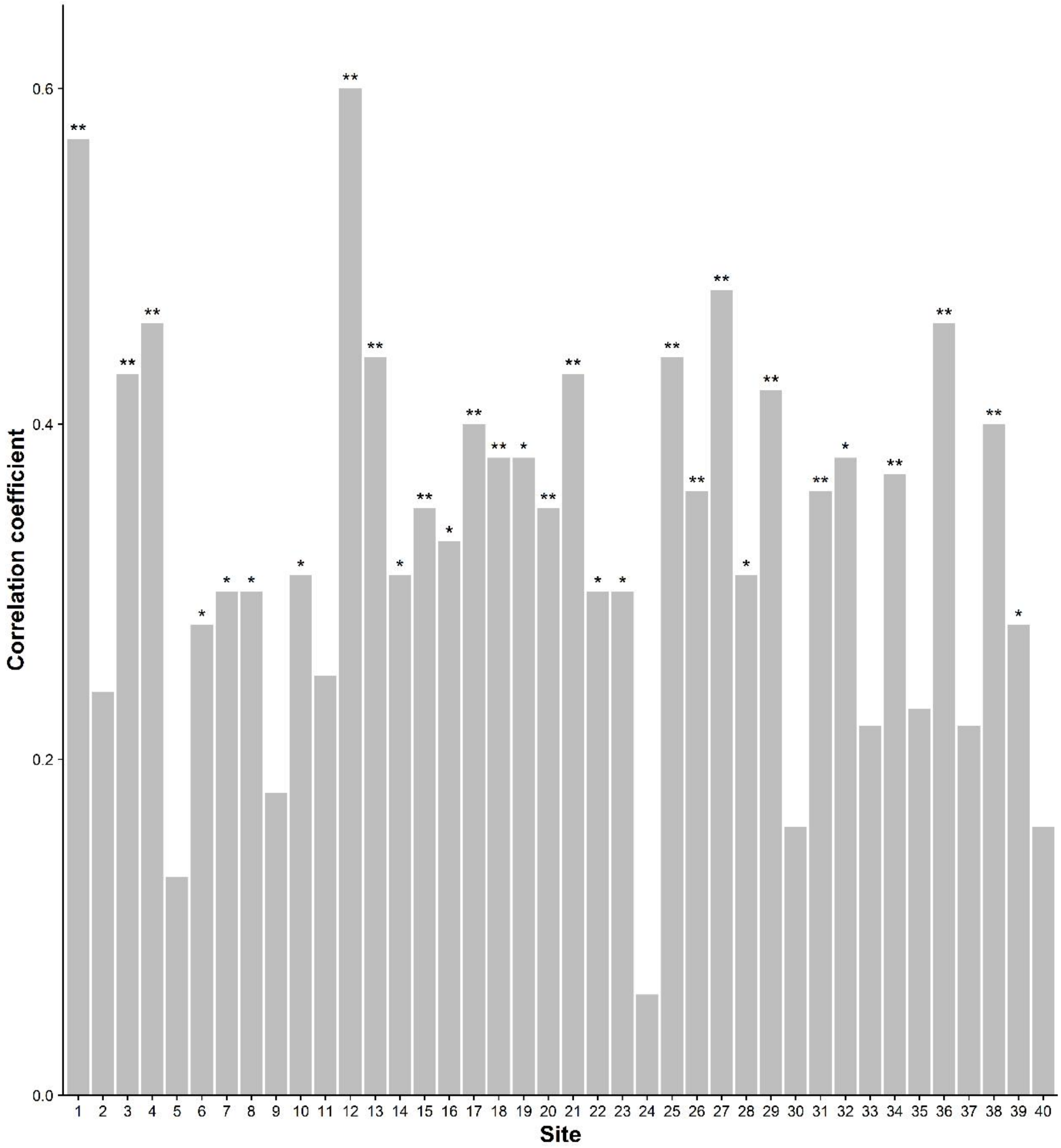

Appendix S6. The correlations of the averaged observed and simulated tree-ring width chronologies, in which (a) radial growth was limited by soil moisture, (b) radial growth was limited by temperature, and (c) radial growth was neither limited by temperature nor soil moisture. The dashed black line and solid grey line represent simulated and actual chronologies, respectively. Values of *r* represent the correlation coefficients between observed and simulated chronologies.

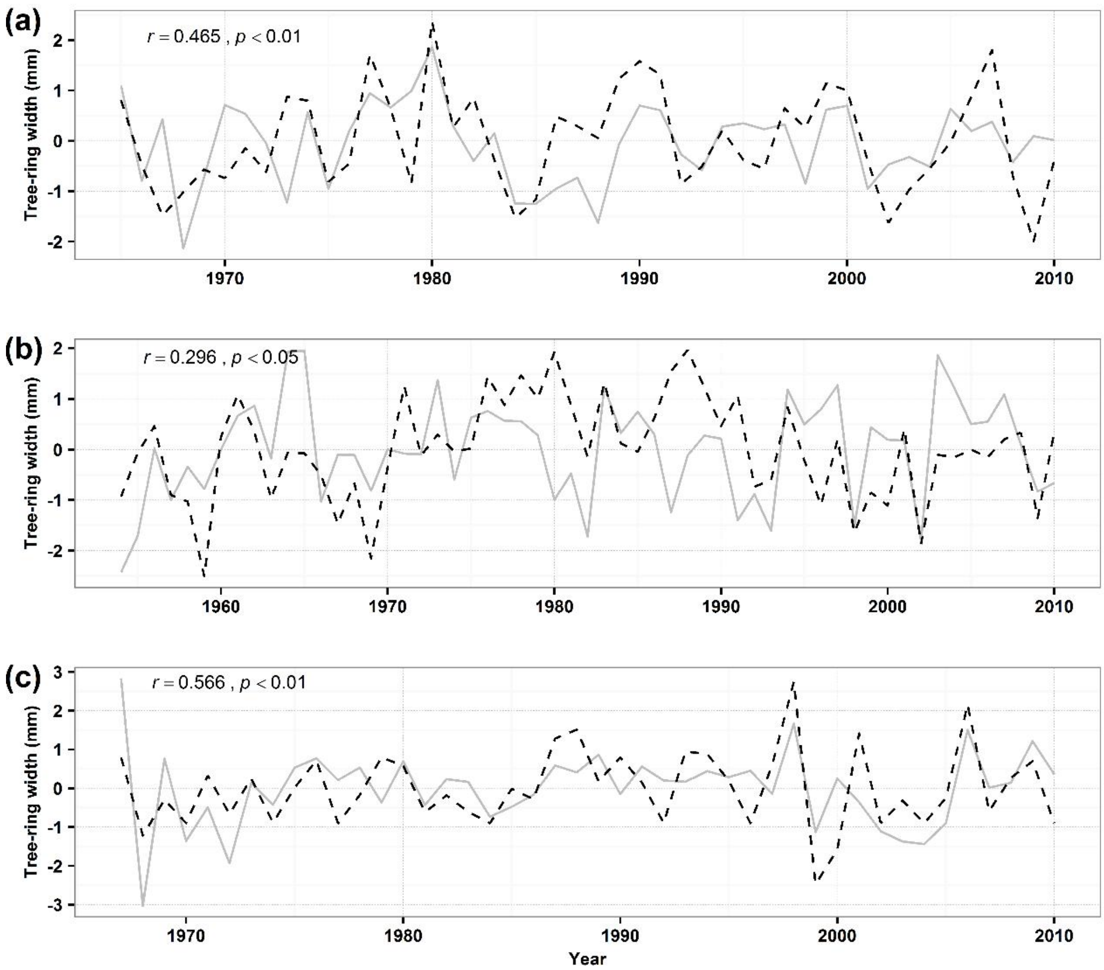

Appendix S7. (a) Variation in the monthly total precipitation from 1930 to 2010; (b) variation in the monthly growing degree days (GDD > 5℃) from 1930 to 2010.

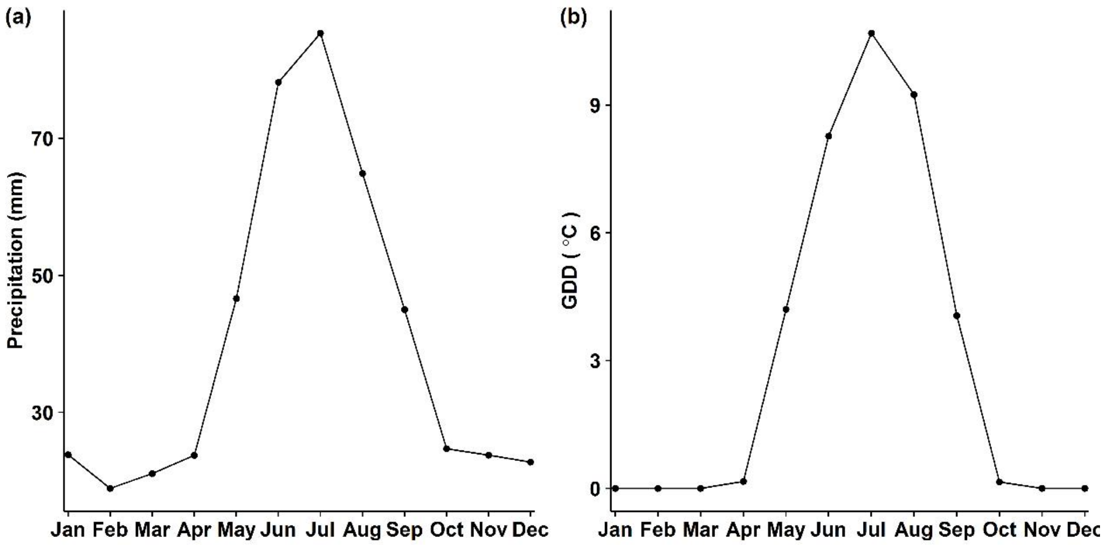

Appendix S8. (a) Difference in the monthly total precipitation between June and July along different latitudes; (b) difference in the monthly mean temperature between June and July along different latitudes. The shaded area presents 95% confidence intervals.